

## Application of Artificial Neural Network in Biotribological Research of Dental Glass Ceramic

M. Pantić<sup>a,b</sup>, A. Đorđević<sup>a,b</sup>, M. Erić<sup>a</sup>, S. Mitrović<sup>a</sup>, M. Babić<sup>a</sup>, D. Džunić<sup>a</sup>, M. Stefanović<sup>a</sup>

<sup>a</sup>University of Kragujevac, Faculty of Engineering, Kragujevac, Serbia,

<sup>b</sup>Higher technical school of professional studies Zvečan, Zvečan, Serbia.

### Keywords:

*Tribological characteristics  
Dental glass ceramic  
Neural networks  
Mathematical modelling*

### ABSTRACT

*A tribological system is a complex non-linear system composed of the elements that are connected structurally and functionally. The aim of this paper is to present an overview of artificial neural networks, its development and applications of neural networks in the prediction of tribological properties of dental glass ceramic using a newly measured ball-on-plate nanotribometer. The possibility of artificial neural networks application to solve complex nonlinear problems and to identify tribological characteristics of dental glass ceramic in terms of wear rate and coefficient of friction are presented in this paper.*

### Corresponding author:

*Aleksandar Đorđević  
University of Kragujevac, Faculty of  
Engineering, Kragujevac, Serbia.  
E-mail: [adjordjevic@kg.ac.rs](mailto:adjordjevic@kg.ac.rs)*

© 2018 Published by Faculty of Engineering

## 1. INTRODUCTION

Application of ANNs has become wider in last few decades, especially in different areas of production engineering. Hence, in tribological experiments, application of ANNs models values has become more present for prediction of tribological properties, i.e. for wear rate and coefficient of friction, according to the defined terms of the contact, for materials that are tested. Neural networks have been used for prediction of short fibre composites tribological properties [1], for prediction of carbon fiber and TiO<sub>2</sub> composites properties [2], plasma nitrided 316L stainless steel tribological properties [3], for prediction of composite PEEK-CF30 tribological behavior [4], etc.

Particular attention of researchers in recent years was occupied by biotribology. Biotribology

is one of the current and rapidly growing field of tribology. The diversity of research activities in biotribology is very large and includes many scientific fields. A large number of papers in various fields of biotribology from year to year are published in numerous prestigious scientific journals [5]. A very important area in recent years that is the focus of numerous studies is the field of research and development of new biomaterials. The term biomaterial refers to materials with such unique characteristics which make them particularly suitable for close contact with the living tissue, and whose production process is often applied, or mimics a biological phenomenon [6]. New nanomaterials such as nanotubes, carbon fibers, nanolegure, as well as various types of polymers, ceramics, or metal alloys and the nanocomposite and a number of other powerful new class of materials are promising extraordinary achievements in

the medical materials and services. Materials, observed at a nano level may show totally different characteristics in relation to those which are manifested on a macro level, thus allowing the unique application. In recent years a numerous areas of health services have progressed to the point that their new approaches to day-to-day raise the patients lifestyles.

Having in mind previously mentioned, ANNs method were identified as appropriate for prediction of tribological parameters of all-ceramic material prepared with different finishing processes. Ceramic is an inorganic, non-metallic material that is solidified by the heating process and has about 30 % of the crystal structure [7]. In dentistry it was always pursued and will be strived to find new materials that have suitable characteristics to replace the natural tooth structure. With the development of science in general and the development of dentistry through various scientific and technical research, aesthetic materials for prosthetic purposes have evolved almost to the extent that their properties meet all necessary requirements in the form of aesthetics, function and biocompatibility [9]. Excellent characteristics enabled the widespread use of ceramics as the restorative in the field of cosmetic dentistry.

In the present research paper experiments were conducted on lithium disilicate ( $\text{Li}_x(\text{SiO}_2)_y$ ) sample. The material is characterized by high values of bending strength and broad application in making restorations and teeth bridges. Based on the idea that the future of all-ceramic systems is to use PRESS (pressing technology) and CAD/CAM technology, a new advanced system called IPS e.max (Ivoclar Vivadent, Liechtenstein) was developed. It embraces the most aesthetic and high-resistant materials intended for the PRESS and CAD/CAM technology. Hence, commercial material IPS e.max CAD lithium disilicate glass ceramics for CAD/CAM systems and the pressing technology were designed. Blocks for CAD/CAM are blue in color, they are molded in one piece and within the metasilicate phase (partially crystallized,  $\text{Li}_2\text{SiO}_3$ ). As raw material, the value of their bending strength is smaller which allows their quick processing in the CAD/CAM system. A crystallization process is performed to obtain a

final form of the crystal of lithium disilicate ( $\text{Li}_2\text{Si}_2\text{O}_5$ ). Therefore, blocks are receiving a significantly higher bending strength with the values of 360 MPa [9].

In this paper, the influence of input nanotribometer parameters, i.e. parameters of the device used for testing tribological characteristics onto the lithium disilicate ( $\text{Li}_x(\text{SiO}_2)_y$ ) sample has been analysed. Artificial neural network approach has been used for mathematical modelling and for identification of input tribometer parameters which led to minimal degree of wear rate and coefficient of friction values.

## 2. EXPERIMENTAL PROCEDURE

Within the tribological tests, the characterization of tribological phenomena, friction and wear, according to the defined terms of the contact, for commercial dental material lithium disilicate IPS e.max CAD are determined. Tribology tests, whose parameters are shown in Table 1, are realized on the CSM nanotribometer (Fig. 1).

**Table 1.** Tribological input parameters [9].

|   |
|---|
| <b>Instrument preferences</b>   |
| - Linear reciprocating module (linear mode acquisition)<br>- Half of amplitude: 0.5 mm<br>- Frequency: 100 Hz<br>- Ambient air temperature: $23 \pm 2$ °C |
| <b>Tested samples</b>   |
| - Commercial lithium disilicate - IPS e.max CAD (Ivoclar Vivadent, Liechtenstein)<br>- Finishing procedures of samples: polishing, glazing and grinding   |
| <b>Static body</b>  |
| - Commercially supplied alumina ball ( $\text{Al}_2\text{O}_3$ )<br>- Ball diameter: 1.5 mm   |
| <b>Normal load values</b>   |
| - $F_n$ : 250 mN; 500 mN; 750 mN; 1000 mN   |
| <b>Sliding speed values</b>   |
| - $v$ : 4 mm/s; 8 mm/s; 12 mm/s   |
| <b>The test duration</b>  |
| - 10.000 cycles (20 m)  |
| <b>Environment contact zone</b>   |
| - Artificial saliva medium  |

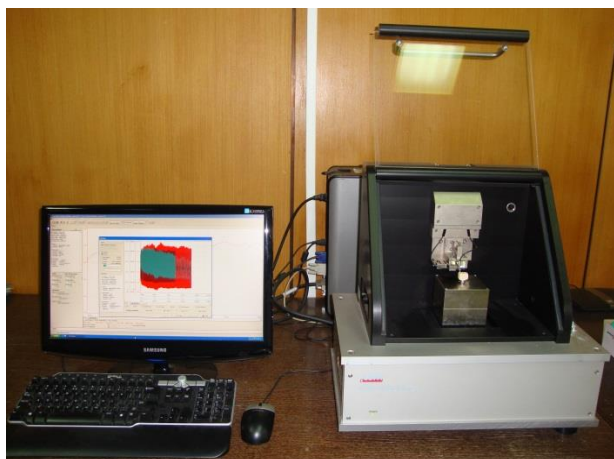


Fig. 1. CSM nanotribometer.

Based on this literature review, it was decided that the tribological test should be carried out in the presence of artificial saliva in the contact zone, in order to more realistically simulate real conditions of the oral environment. The results of the in vitro wear test, which were conducted in [10], showed that the artificial saliva could also have the effect of cooling and lubrication during the wear process. Also, the risk of damage to the contact surfaces of the materials can be significantly reduced in the region of artificial saliva, compared with a dry state. Lubrication mechanism saliva is based on the complete separation of the sliding surfaces in contact with a thin layer of saliva [11].



Fig. 2. Crystallized samples of lithium disilicate IPS e.max CAD, prepared with 3 different finishing procedures.

The contact elements of tribomechanical system are samples of lithium disilicate prepared with three different finishing procedures: polishing, glazing and grinding and commercial alumina ball ( $Al_2O_3$ ) with the diameter of 1.5 mm. It is

generally known that the alumina has an ultra-high hardness with the value 9, according to Mohs scale [12], immediately behind the diamond, and excellent wear resistance. Prepared samples are in the shape of a block (18 mm length, 14 mm width and 12 mm height), Fig. 2.

Tribological tests were intended for tracking of wear and friction values, depending on the sliding distance. During the tests, the coefficient of friction values were recorded in real time, by applying TRIBOX 2.9.0. software. After each test, the sample was removed from nanotribometer and the image of wear tracks were recorded with optical microscope. Wear of the contact surface material was measured by the average area of a wear track with software tools, based on optical images. Wear volume and wear rate were calculated for each test, according to ASTM G133-05 Standard, after the total sliding distance by 20 m. Wear rate ( $W$ ) was calculated according to the following equation [13]:

$$W=V/S, [mm^3/m] \quad (1)$$

where:  $V$  – wear volume of material [ $mm^3$ ], and  $s$  – sliding distance [m]. Wear rate was calculated for each test.

### 3. ARTIFICIAL NEURAL NETWORK MODELLING OF WEAR RATES AND COEFFICIENT OF FRICTION

More or less similar to real biological neural networks, ANNs are made up of interconnected, simple processing elements called artificial neurons. When they process information, the processing elements in the NN operate simultaneously and collectively, like biological neurons. ANNs have the required properties similar to those which possess the biological neural network, such as the ability to learn, to be self-organized and support the robustness [14]. Similarly to biological neuron, each ANN neuron receives the inputs, processes them and delivers the outputs. The inputs can be an input set of data or the output from another neuron. The output can be the final result, or may be input to another neuron. In biological neurons and synapses, there are different strengths of synaptic transmission, and intensities in the neurons, in the ANN these strengths are represented as the values of the weight coefficients. These neurons are grouped in layers. Each ANN contains only one input layer,

zero or more hidden layers and one output layer. The most frequently applied structure of the ANN is a neural network consisting of three layers, all the layers except the input layer contain neurons. Number of inputs in ANN, corresponds to the number of defined independent parameters used for prediction, while the number of neurons in the output layer is equal to the number of dependent parameters whose values should be predicted. There is a direct ANN proportions between the number of hidden layers and the number of neurons in them and ANN capabilities to approximate complex functions. This does not mean that the networks with more complex structures work better. The reason for poor performance in these cases is linked to the fact that the complicated ANNs are more sensitive to noises that exist in the input data. It is necessary to make a compromise between the approximate ANNs capabilities and noises that are entered by the input data.

The power of neural network models lies in the fact that the weights  $w$  and biases  $b$  can be adjusted. Weights adjustment procedure is based on a specific data set and it is called ANN training with a certain data set (training set). The basic idea of training is to adapt the data network, i.e. to determine the relations that exist between the independent and dependent data in the training set. Using a custom network in future situations (for new data) is possible on the basis of previously established relationships and network capacity to generalize these relations to a broader group and thus reach possible conclusions.

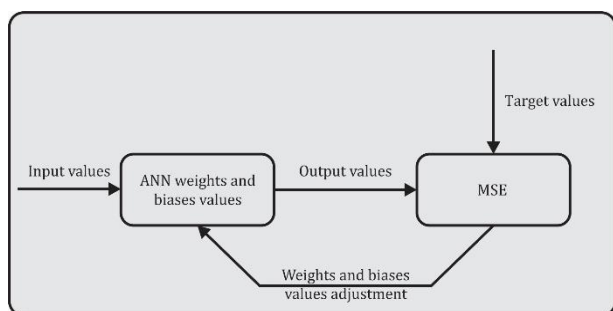


**Fig. 3.** General framework of ANN training process.

ANN training is presented at the Fig. 3. The present sample consists of two parts of the input and the target data portion (supervised learning). Initially, the network weight coefficients have assigned random values (usually in the range of -1 to 1). The input part of

the first sample is put into the network. Network calculates the output on the basis of: the value of weight and biases, the number of layers that are in incorporated, and the type and quantity of neurons in each layer. The output value from the network is compared with the target value of the sample and the weights values of the network are adjusted, so that the metric, which describes the distance between the target value and outputs, is minimized.

The parameters that are associated with training algorithms, that should be appointed, are: error function, learning rate and number of iterations. Error function is used to measure the difference between the target value and output values of the network. The values of ANN weights are updated in the direction that makes the error function to be minimized. Frequently used functions are Mean Square Error (MSE) and Mean Absolute Error (MAE). For training and testing of ANN, MSE is commonly applied. MSE may be used as a target function to be minimized, in order to obtain optimal initial values of the ANN weight coefficients [15].

There are two basic types of ANN training, which are incremental and serial training. In the context of the incremental training weights and biases of the ANN are adjusted each time when one of the input samples is introduced to the ANN, while in the serial training, connection weights of ANN neurons are adjusted only when all the input samples are introduced into the network [16]. The cycle of bringing the entire training set in an ANN is called an epoch, a number of cyclical repetitions is the characteristic of the ANN, called the total number of epochs.

The updating mechanism of the ANN weights value is called a training algorithm. There are several training algorithms proposed in the literature [17-19]. The most commonly used training algorithm is related to the feed-forward ANN. ANN is characterized as a feed-forward network, if it is possible to connect the input layer to the hidden layers and the output layer, in a way that the each neuron is only associated with neurons from the preceding layers. All the algorithms use the MSE function to adjust the values of the weight coefficients and biases, so that the MSE function is minimized. The value of MSE function is determined by applying the back propagation techniques. Backpropagation is a

mechanism of ANN learning, this is an iterative process in which the difference between the outputs of the network and the target values are given back into the ANN, so that the values of ANN weights coefficients and biases are gradually adapted to create output values that are closer to the target values [15].

In this paper, the three layered feed-forward backpropagation ANN architecture has been proposed for modelling. The input layer of the ANN model consists of two neurons corresponding to the two tribological parameters that were varied in the experiments, normal force ( $F$ ) and sliding speed ( $v$ ) and the output layer has one neurons for prediction of wear rate ( $W$ ) or coefficient of friction ( $\mu$ ). Due to the different finishing procedures of samples (polished, glazed and grinded surfaces) and number of parameters that have to be predicted ( $W$  and  $\mu$ ), six different ANN models were determined, one for each finishing procedure and parameter.

For all six ANN models, the entire experimental data set ( $N_{tot}=12 \times n \times m$ ) was divided into a six data subsets for different parameters prediction ( $n=2$ ) and different conditions ( $m=3$ ). After this, data were further divided within each of six subsets into a data subset for training, a data subset for validation and a data subset for testing. 50 % of randomly selected data have been employed for training, 25 % for validation and 25 % for testing, separately for each of the six subsets of experimental data.

Main problems that could occur in backpropagation are ANNs overfitting and overtraining. Overtraining means that ANN only memorizes the training data set and learns these data excellently but doesn't have an ability to generalize to new data and because of that performance of the validation set decreases [20]. Having this in mind, the objective is to determine the compatible ANN

model that has the total MSE acceptably low [21,22]. Selected ANN architecture had one hidden layer with ten neurons for prediction and biotribological process modelling. It has been presumed that this architecture could obtain minimal MSE value, between the output values and real experimental target data. Two different functions have been used as a transfer function; from the input to a hidden layer, it has been transigmoid function, and between hidden and output layer, it has been pure linear function. Prior to ANN training, the training data were normalized within the range [-1 1] and the initial weights values were adopted according to Nguyen-Widrow method.

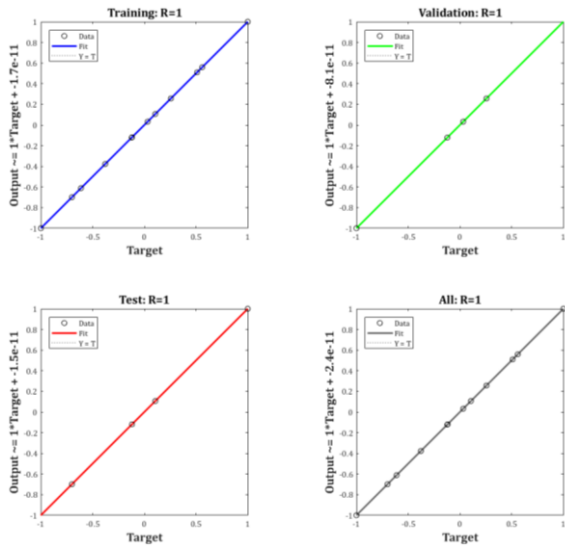
The performance of the network was measured by the MSE of the predicted outputs with regards to the real experimental target data. The goal is to get MSE as close as possible to zero. The zero means that there is no error between outputs of the network and target values. In this case, ANN model trainings were initially set to terminate after a maximum number of epochs, but they were stopped after a certain number of epochs since no further improvement in the MSE was achieved. MSE values were obtained after trainings, validations and testing of ANN models and they are shown in Table 2.

Except MSE another performance measure for ANN model is correlation coefficient (R). This is a statistical measure of the strength of correlation between predicted and experimental values. A perfect correlation is obtained when  $R=1$ . A suitable ANN model should have the correlation coefficient greater than 0.8. Correlation coefficients of the developed wear rate prediction ANN models for all three differently processed surfaces are shown in Fig. 4.

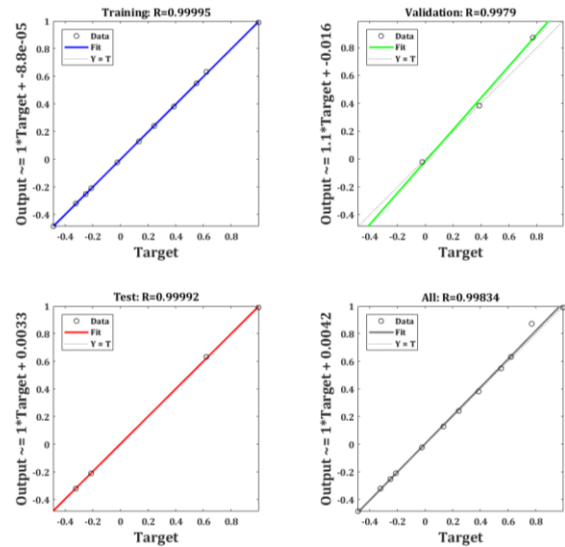
Similarly to the previous correlation coefficients of the developed coefficient of friction prediction, ANN models for all three differently processed surfaces are shown in Fig. 5.

**Table 2.** MSE values of ANN model.

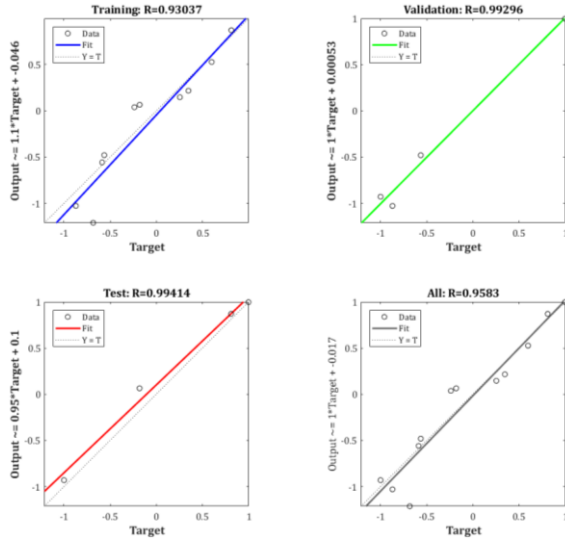
| Model no. | ANN architecture | Mean Squared Error (MSE) |            |         | No. of epochs |
|-----------|------------------|--------------------------|------------|---------|---------------|
|           |                  | Training                 | Validation | Testing |               |
| M 1       | 2-10-1           | 0.0014                   | 0.011220   | 0.0213  | 4             |
| M 2       | 2-10-1           | 0.0004                   | 0.003248   | 0.001   | 3             |
| M 3       | 2-10-1           | 0.0000                   | 0.006359   | 0.0011  | 6             |
| M 4       | 2-10-1           | 0.0012                   | 0.000311   | 0.0021  | 4             |
| M 5       | 2-10-1           | 0.0001                   | 0.000070   | 0.0075  | 5             |
| M 6       | 2-10-1           | 0.0028                   | 0.003130   | 0.0059  | 5             |



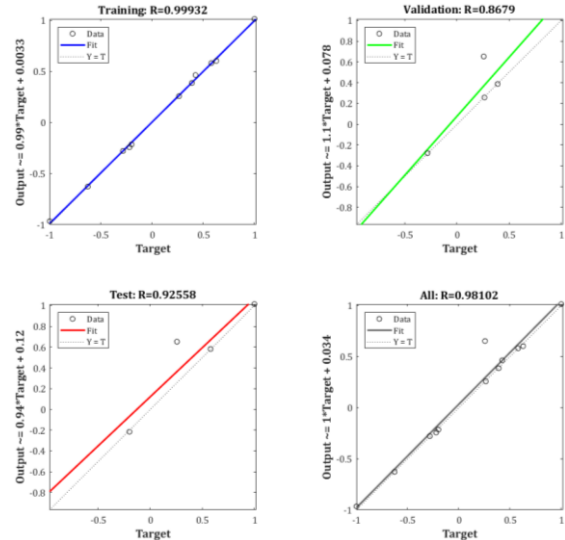
a) polished surface



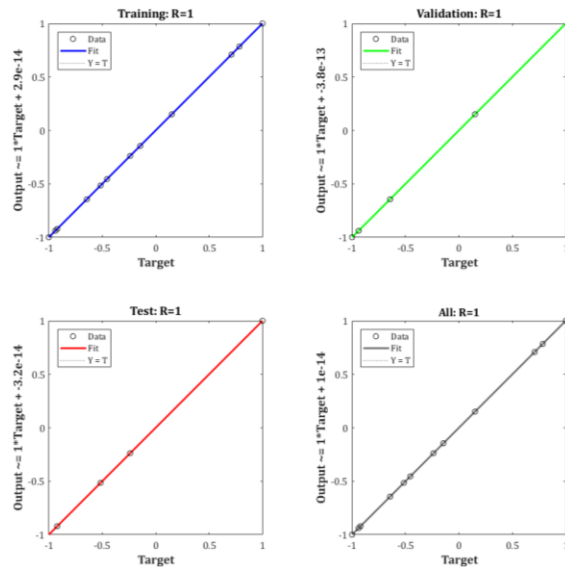
a) polished surface



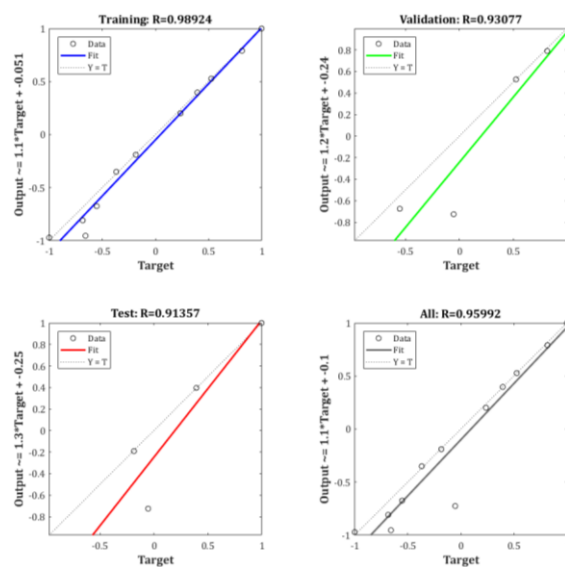
b) glazed surface



b) glazed surfaces



c) grinded surface



c) grinded surface

**Fig. 4.** Correlation between predicted and experimental data during training, validation and testing of the developed ANN model for wear rate.

**Fig. 5.** Correlation between predicted and experimental data during training, validation and testing of the developed ANN model for coefficient of friction.

The weights and biases of the wear rate ANN model with polished surface that were determined in training process are given in Table 3, for other models values are determined in a similar manner.

**Table 3.** The weights and biases of developed ANN model for polished surface wear rate prediction.

| Weights  |          | Biases  |         |          |
|----------|----------|---------|---------|----------|
| $w_{ji}$ | $w_{kj}$ | $b_j$   | $b_k$   |          |
| 2.9459   | -3.1857  | 0.21534 | -4.5085 | -0.21755 |
| 3.0566   | 3.1389   | -0.0533 | -3.5304 |          |
| -3.0417  | 2.9174   | 0.42509 | 2.8794  |          |
| 4.3825   | 0.09847  | 0.52473 | -1.559  |          |
| 1.8201   | 4.0076   | 0.27768 | -0.5393 |          |
| -2.9782  | -3.2504  | 0.46395 | -0.9972 |          |
| -4.1289  | -1.5583  | -0.3946 | -1.4537 |          |
| 0.50834  | 4.3896   | 0.10039 | 2.4669  |          |
| 3.5561   | 1.9841   | 0.57493 | 3.8784  |          |
| 3.2914   | 3.5083   | -0.3414 | 3.9908  |          |

Using the weights and biases from Table 3 and in accordance with selected ANN architecture the exact mathematical relationship between tribological response, Wear rate ( $W$ ), coefficient of friction ( $\mu$ ) and input parameters, normal force ( $F$ ) and sliding speed ( $v$ ) in different finishing procedures, can be expressed by the following Equations 2 and 3. In these equation  $X$  is the column vector which contains normalized values of  $F$  and  $v$  and  $w_{norm}$  and  $\mu_{norm}$  are the normalized value for the  $W$  and  $\mu$  for each of the defined contact conditions. To obtain actual values of wear rate and coefficient of friction, it is necessary to denormalize the obtained output values.

$$w_{norm} = \left[ \frac{2}{1+e^{-2(X \cdot w_{ji} + b_j)}} - 1 \right] \cdot w_{kj} + b_k \quad (2)$$

$$\mu_{norm} = \left[ \frac{2}{1+e^{-2(X \cdot w_{ji} + b_j)}} - 1 \right] \cdot w_{kj} + b_k \quad (3)$$

The next section provides an overview of measured and predicted values of the wear rate and coefficient of friction, within the framework of tribological tests, according to the previously defined contact surfaces of samples.

#### 4. RESULTS

Using Equation 2 and 3 and by varying values of both input parameters, the effects of tribological tests on the wear rate and coefficient of friction were analyzed. Hence, comparisons of actual target data and those predicted by developed ANN models were obtained. Results are shown in Tables 4 and 5.

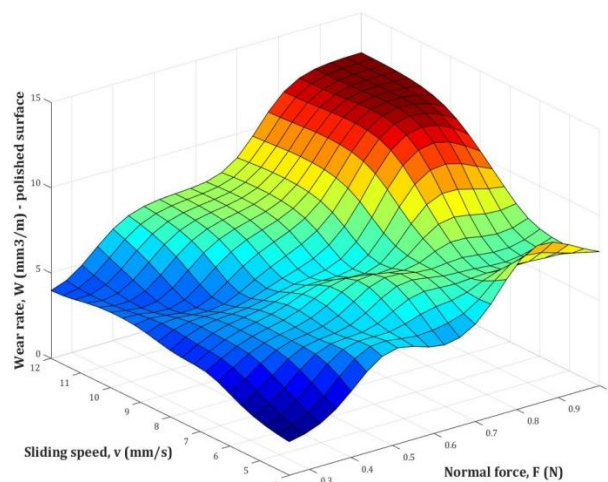
**Table 4.** The real and predicted values of the wear rate of lithium disilicate (*IPS e.max CAD*).

| Wear rate, $W$   |           |             |                      |
|------------------|-----------|-------------|----------------------|
| Polished surface |           |             |                      |
| $F_n, N$         | $v, mm/s$ | Real values | ANN predicted values |
| 0.25             | 4         | 1.893       | 1.97743              |
|                  | 8         | 3.512       | 3.89983              |
|                  | 12        | 3.983       | 3.97447              |
| 0.5              | 4         | 5.244       | 5.60719              |
|                  | 8         | 6.617       | 5.40687              |
|                  | 12        | 7.446       | 7.4358               |
| 0.75             | 4         | 6.635       | 6.99912              |
|                  | 8         | 8.653       | 8.72522              |
|                  | 12        | 10.013      | 9.98442              |
| 1                | 4         | 7.846       | 7.85105              |
|                  | 8         | 10.279      | 10.302               |
|                  | 12        | 12.648      | 12.6478              |
| Glazed surfaces  |           |             |                      |
| $F_n, N$         | $v, mm/s$ | Real values | ANN predicted values |
| 0.25             | 4         | 1.905       | 1.905                |
|                  | 8         | 3.240       | 3.23984              |
|                  | 12        | 3.744       | 3.74389              |
| 0.5              | 4         | 2.449       | 2.44915              |
|                  | 8         | 5.363       | 5.36283              |
|                  | 12        | 7.203       | 6.82267              |
| 0.75             | 4         | 3.647       | 3.64679              |
|                  | 8         | 7.592       | 7.59199              |
|                  | 12        | 9.553       | 9.55301              |
| 1                | 4         | 5.122       | 5.12221              |
|                  | 8         | 8.655       | 8.65501              |
|                  | 12        | 10.348      | 10.348               |
| Grinded surface  |           |             |                      |
| $F_n, N$         | $v, mm/s$ | Real values | ANN predicted values |
| 0.25             | 4         | 0.028       | 0.028                |
|                  | 8         | 0.084       | 0.084001             |
|                  | 12        | 0.100       | 0.099999             |
| 0.5              | 4         | 0.352       | 0.351996             |
|                  | 8         | 0.469       | 0.469004             |
|                  | 12        | 0.524       | 0.523996             |
| 0.75             | 4         | 0.721       | 0.721001             |
|                  | 8         | 0.806       | 0.806005             |
|                  | 12        | 1.075       | 1.075001             |
| 1                | 4         | 1.582       | 1.581998             |
|                  | 8         | 1.651       | 1.650994             |
|                  | 12        | 1.848       | 1.848                |

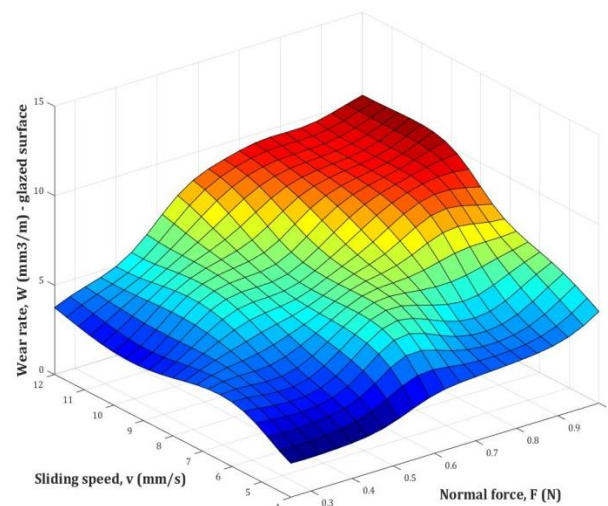
**Table 5.** The real and predicted values of the coefficient of friction of lithium disilicate (*IPS e.max CAD*).

| Coefficient of friction, $\mu$ |            |             |                      |
|--------------------------------|------------|-------------|----------------------|
| Polished surface               |            |             |                      |
| $F_n$ , N                      | $v$ , mm/s | Real values | ANN predicted values |
| 0.25                           | 4          | 0.441       | 0.441                |
|                                | 8          | 0.406       | 0.406                |
|                                | 12         | 0.372       | 0.372                |
| 0.5                            | 4          | 0.383       | 0.383                |
|                                | 8          | 0.347       | 0.347                |
|                                | 12         | 0.308       | 0.308                |
| 0.75                           | 4          | 0.325       | 0.32501              |
|                                | 8          | 0.284       | 0.284                |
|                                | 12         | 0.255       | 0.255                |
| 1                              | 4          | 0.249       | 0.249                |
|                                | 8          | 0.238       | 0.238                |
|                                | 12         | 0.213       | 0.213                |
| Glazed surfaces                |            |             |                      |
| $F_n$ , N                      | $v$ , mm/s | Real values | ANN predicted values |
| 0.25                           | 4          | 0.419       | 0.419                |
|                                | 8          | 0.359       | 0.359                |
|                                | 12         | 0.332       | 0.332                |
| 0.5                            | 4          | 0.366       | 0.366                |
|                                | 8          | 0.337       | 0.337                |
|                                | 12         | 0.314       | 0.314                |
| 0.75                           | 4          | 0.313       | 0.313                |
|                                | 8          | 0.248       | 0.248                |
|                                | 12         | 0.236       | 0.236                |
| 1                              | 4          | 0.245       | 0.24499              |
|                                | 8          | 0.187       | 0.187                |
|                                | 12         | 0.134       | 0.134                |
| Grinded surface                |            |             |                      |
| $F_n$ , N                      | $v$ , mm/s | Real values | ANN predicted values |
| 0.25                           | 4          | 0.247       | 0.247                |
|                                | 8          | 0.240       | 0.24                 |
|                                | 12         | 0.195       | 0.195                |
| 0.5                            | 4          | 0.229       | 0.229                |
|                                | 8          | 0.218       | 0.218                |
|                                | 12         | 0.188       | 0.188                |
| 0.75                           | 4          | 0.224       | 0.224                |
|                                | 8          | 0.207       | 0.207                |
|                                | 12         | 0.184       | 0.184                |
| 1                              | 4          | 0.202       | 0.202                |
|                                | 8          | 0.183       | 0.183                |
|                                | 12         | 0.171       | 0.171                |

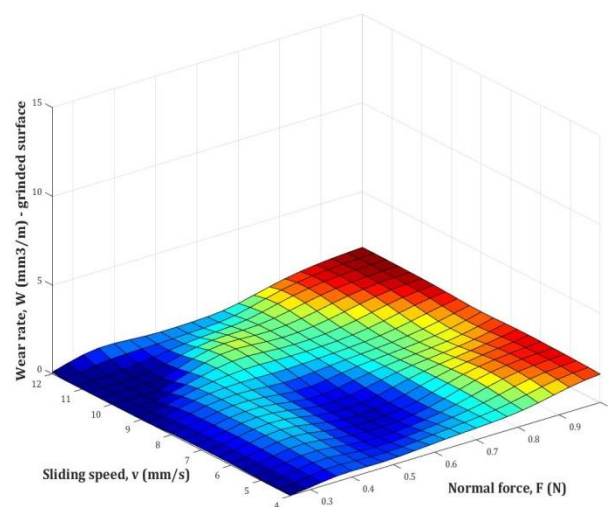
Analysing the experimental data, the area of parameters combinations for  $F$  and  $v$  was defined. This area was shown in Figs. 6 and 7.



a) polished surface



b) glazed surfaces



c) grinded surface

**Fig. 6.** Influence of the F-v interaction on the wear rate ( $W$ ).



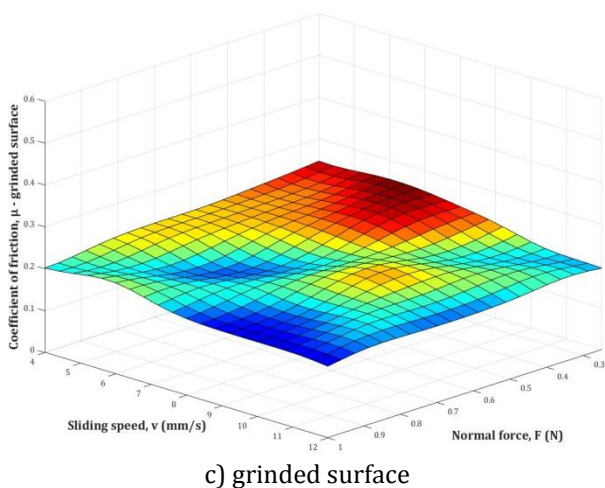
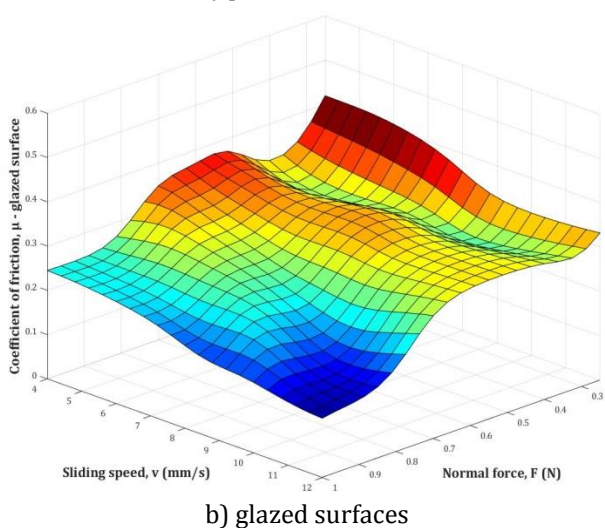
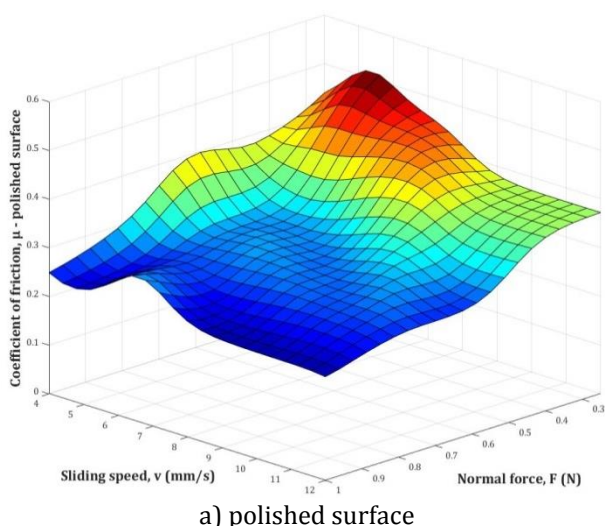


**Fig. 7.** Influence of the F-v interaction on the coefficient of friction ( $\mu$ ).

From Figs. 4 and 5, it can be concluded that higher values of normal force ( $>0.8$  N) and sliding speed ( $>8$  mm/s) lead to higher values of wear rate ( $W$ ), while the lower values of normal force ( $<0.4$  N) and sliding speed ( $<8$  mm/s) lead to higher values of coefficient of friction ( $\mu$ ).

Having this in mind, it is necessary to further optimize the input values in order to obtain preferred outputs.

## 5. CONCLUSIONS

In this paper a mathematical modelling of wear rate and coefficient of friction in tribological process of dental glass ceramic were introduced. This was performed using ANN models for different surface conditions. ANNs have proven to be suitable due to their potential to learn nonlinear features of any system from incomplete experimental data regardless of external noise. Model was verified using tribological experimental values obtained by means of nanotribometer. Beside that, a comparison between experimental and predicted values was conducted. These indices showed that the models were quite acceptable for all defined conditions. Created model was used to describe the influence of input tribological parameters such as normal force and sliding speed on analyzed material wear rate and coefficient of friction. According to this the plots were created that can be used to identify biotribological conditions that may lead to minimal wear rate or coefficient of friction.

Future research will take in consideration other materials and conditions, or the application of an optimization method used for optimal values achievement of wear rate or coefficient of friction. Their values will be included in mathematical modelling procedure to obtain a complete view of output tribological properties.

## Acknowledgement

Research presented in this paper was supported by Ministry of Education, Science and Technology Development of Republic of Serbia, Grant TR 35021.

## REFERENCES

- [1] Z. Zhang, K. Friedrich, K. Velten, *Prediction on tribological properties of short fibre composites using artificial neural networks*, Wear, vol. 252, iss. 7-8, pp. 668-675, 2002, doi: [10.1016/S0043-1648\(02\)00023-6](https://doi.org/10.1016/S0043-1648(02)00023-6)

- [2] J. Zhu, Y. Shi, X. Feng, H. Wang, X. Lu, *Prediction on tribological properties of carbon fiber and TiO<sub>2</sub> synergistic reinforced polytetrafluoroethylene composites with artificial neural networks*, Materials & Design, vol. 30, iss. 4, pp. 1042-1049, 2009, doi: [10.1016/j.matdes.2008.06.045](https://doi.org/10.1016/j.matdes.2008.06.045)
- [3] A. Yetim, M. Codur, M. Yazici, *Using of artificial neural network for the prediction of tribological properties of plasma nitrided 316L stainless steel*, Materials Letters, vol. 158, pp. 170-173, 2015, doi: [10.1016/j.matlet.2015.06.015](https://doi.org/10.1016/j.matlet.2015.06.015)
- [4] X. LiuJie, J. Davim, R. Cardoso, *Prediction on tribological behaviour of composite PEEK-CF30 using artificial neural networks*, Journal of Materials Processing Technology, vol. 189, iss. 1-3, pp. 374-378, 2007, doi: [10.1016/j.jmatprotec.2007.02.019](https://doi.org/10.1016/j.jmatprotec.2007.02.019)
- [5] Z. Zhou, H. Yu, J. Zheng, L. Qian, Y. Yan, *Dental Biotribology, 1st ed.* New York, NY: Springer New York, 2013.
- [6] T. Larsson, M. Martinez, J. Valles, *Biomaterials for Healthcare. A decade of EU-funded research*, European Commission, Directorate – General for Research, Industrial technologies, Unit G3, Value – Added Materials, 2007.
- [7] H. Hennicke, *Zum Begriff Keramik und zur Einteilung keramischer Werkstoffe*, Berichte der Deutschen Keramischen Gesellschaft, vol. 44, pp. 209-211, 1967.
- [8] M. Pantić, S. Mitrović, M. Babić, D. Jevremović, T. Kanjevac, D. Džunić, D. Adamović, *AFM Surface Roughness and Topography Analysis of Lithium Disilicate Glass Ceramic*, in 14th International Conference on Tribology, Serbiatrib '15, Belgrade, 2015, pp. 514-521.
- [9] M. Pantić, *Tribological characterization of advanced dental materials*, PhD, University of Kragujevac, Faculty of Engineering, 2017.
- [10] Z. Zhou, J. Zheng, *Oral tribology*, Proceedings of the Institution of Mechanical Engineers, Part J: Journal of Engineering Tribology, vol. 220, no. 8, pp. 739-754, 2006.
- [11] I. Hahn Berg, M. Rutland, T. Arnebrant, *Lubricating Properties of the Initial Salivary Pellicle — an AFM Study*, Biofouling, vol. 19, no. 6, pp. 365-369, 2003, doi: [10.1080/08927010310001618571](https://doi.org/10.1080/08927010310001618571)
- [12] S. Mukherjee, *Applied mineralogy, 1st ed.* Dordrecht: Springer, 2011.
- [13] I. Hutchings, *Tribology: Friction and Wear of Engineering Materials, 1st ed.* Michigan, United States: Edward Arnold Publishers Ltd, University of Michigan, 1992.
- [14] S. Li, D. Wunsch, E. O'Hair, M. Giesselmann, *Comparative Analysis of Regression and Artificial Neural Network Models for Wind Turbine Power Curve Estimation*, Journal of Solar Energy Engineering, vol. 123, no. 4, pp. 327-332, 2001, doi: [10.1115/1.1413216](https://doi.org/10.1115/1.1413216)
- [15] Y. Chang, J. Lin, J. Shieh, M. Abbod, *Optimization the Initial Weights of Artificial Neural Networks via Genetic Algorithm Applied to Hip Bone Fracture Prediction*, Advances in Fuzzy Systems, vol. 2012, p. 9, 2012, doi: [10.1155/2012/951247](https://doi.org/10.1155/2012/951247)
- [16] S. Kumar, *Neural networks: a classroom approach, 1st ed.* New York City, NY: McGraw-Hill Education, 2004.
- [17] A. Askarzadeh, A. Rezazadeh, *Artificial neural network training using a new efficient optimization algorithm*, Applied Soft Computing, vol. 13, iss. 2, pp. 1206-1213, 2013, doi: [10.1016/j.asoc.2012.10.023](https://doi.org/10.1016/j.asoc.2012.10.023)
- [18] S. Panda, A. Sarangi, S. Panigrahi, *A new training strategy for neural network using shuffled frog-leaping algorithm and application to channel equalization*, AEU - International Journal Of Electronics And Communications, vol. 64, iss. 11, pp. 1031-1036, 2014, doi: [10.1016/j.aeue.2014.05.005](https://doi.org/10.1016/j.aeue.2014.05.005)
- [19] V. Chandwani, V. Agrawal, R. Nagar, *Modeling slump of ready mix concrete using genetic algorithms assisted training of Artificial Neural Networks*, Expert Systems with Applications, vol. 42, iss. 2, pp. 885-893, 2015, doi: [10.1016/j.eswa.2014.08.048](https://doi.org/10.1016/j.eswa.2014.08.048)
- [20] I. Peko, B. Nedić, A. Đorđević, D. Džunić, M. Janković, I. Veža, *Modeling of Surface Roughness in Plasma Jet Cutting Process of Thick Structural Steel*, Tribology in Industry, vol. 38, no. 4, pp. 522-529, 2016.
- [21] S.G. Tzafestas, P.J. Dalianis, G. Anthopoulos, *On the overtraining phenomenon of backpropagation neural networks*, Mathematics and Computers in Simulation, vol. 40, iss. 5-6, pp. 507-521, 1996, doi: [10.1016/0378-4754\(95\)00003-8](https://doi.org/10.1016/0378-4754(95)00003-8)
- [22] L. Prechelt, *Automatic early stopping using cross validation: quantifying the criteria*, Neural Networks, vol. 11, iss. 4, pp. 761-767, 1998, doi: [10.1016/S0893-6080\(98\)00010-0](https://doi.org/10.1016/S0893-6080(98)00010-0)